

Seismic Active Earth Pressure Behind the Inclined Retaining Wall for Inclined $c-\phi$ Soil Backfill

Ashish Gupta^{1*} and Vishwas Abhimanyu Sawant²

1. Research Scholar, Department of Civil Engineering, Indian Institute of Technology Roorkee, Roorkee - 247 667, India, * Corresponding Author; email: shi_g2000@rediffmail.com

2. Associate Professor, Department of Civil Engineering, Indian Institute of Technology Roorkee, Roorkee - 247 667, India

Received: 24/08/2018

Accepted: 06/05/2019

ABSTRACT

Keywords:

Pseudo-dynamic approach; Inclined retaining wall; Seismic active earth pressure; Inclined cohesive soil backfill; Soil amplification factor

In the seismically active zones, pseudo-static and pseudo-dynamic approaches are widely used for designing the retaining wall with $c-\phi$ backfill. However, the effect of soil amplification is neglected while considering propagation of waves from base. Soil amplification is crucial in the computation of seismic active earth pressure while analyzing the retaining walls of significant height. It should not be ignored in the seismic design of retaining wall. In this paper, soil amplification effects has been incorporated in the pseudo-dynamic approach for prediction of earth pressure on inclined retaining supporting inclined $c-\phi$ soil backfill. Depth of tension crack has been obtained from derived seismic earth pressure distribution for soils having nonzero cohesion. Then total seismic earth pressure is computed from integration of earth pressure from depth of tensile crack to base. A parametric study is conducted to examine the effect of various parameters like cohesion value of soil backfill, wall friction, wall inclination, soil backfill inclination, soil amplification, horizontal and vertical seismic coefficients. The results obtained for seismic active earth pressure is clearly showing the non-linear behavior behind the inclined retaining wall, which is the requirement of the design of retaining wall in earthquake-prone regions.

1. Introduction

The critical study of the design of retaining wall under seismic condition is very crucial in active seismic zones. The fundamental approach to determine the seismic earth pressure by considering inertia forces of failure wedge due to the ground acceleration was suggested by Okabe [1] and Mononobe and Matsuo [2]. This approach is known as pseudo-static method or M-O Method. Pseudo-static method is mostly used by many researchers to analyze the retaining walls in seismic zones. In this approach, only maximum values of inertia forces are considered neglecting time dependency. All response parameters and forces are

considered in phase without any time lag. This is one of the major limitations of this approach.

To overcome the deficiencies of pseudo-static method to analyze the retaining walls, Steedman and Zeng [3] had developed a new approach called the pseudo-dynamic approach. The approach considers the propagation of finite shear waves from the base in upward direction. Choudhury and Nimbalkar [4-5] had extended the pseudo-dynamic approach by including primary wave propagation to include vertical inertia forces in the analysis. These studies have focused only vertical wall. Nimbalkar and Choudhury [6] included the soil

amplification effect in the pseudo-dynamic approach to determine the seismic earth pressure behind the vertical retaining wall. Ghosh [7] had extended the approach developed by Nimbalkar and Choudhury [6] to include wall inclination. Considering inclined wall and inclined backfill, Gupta and Sawant [8] had presented a detailed parametric study to highlight the effect of soil amplification on the dynamic response of retaining wall.

Considering the soil backfill as $c-\phi$ soil, Ghosh and Sharma [9] had analyzed the retaining wall using the pseudo-dynamic approach. The effect of tension crack in the top portion of $c-\phi$ soil backfill was reported in this study. However, the tension crack was determined by the Rankine's analysis of active earth pressure for $c-\phi$ soil backfill under static case. To investigate the effect of tension crack in the top portion of $c-\phi$ soil backfill under seismic condition, Shao-jun et al. [10] extended the study of Ghosh and Sharma [9] without considering the soil amplification. In this paper, soil amplification effects has been incorporated in the pseudo-dynamic approach for prediction of earth pressure on inclined retaining supporting inclined $c-\phi$ soil backfill. Depth of tension crack has been obtained from derived seismic earth pressure distribution for soils having nonzero cohesion.

2. Proposed Method of Analysis

The retaining wall AB of height H is inclined at an angle θ with the vertical as shown in Figure (1). The soil backfill is inclined at an angle i with the

horizontal. The wall friction angle is δ . The soil backfill retaining is having cohesion c and soil friction angle ϕ . The unit weight of backfill is γ . Shear waves with velocity V_s and primary waves with velocity V_p are assumed to propagate upward from the base. The effect of soil amplification is incorporated by assuming linear variation in the input ground acceleration along depth within the soil media. The horizontal and vertical seismic acceleration of base of the retaining wall is assumed as $a_h = k_h g$ and $a_v = k_v g$. The values of a_h and a_v at the top has been assumed to be greater than the values at the base. The horizontal and vertical seismic coefficient at the top of the retaining wall is taken as $k_{h(z=0)} = f_a \cdot k_{h(z=H)}$ and $k_{v(z=0)} = f_a \cdot k_{v(z=H)}$, where f_a is the soil amplification factor. In the present study, a period of lateral shaking is taken as $T=2\pi/\omega$, where ω is the angular frequency.

ABE is the assumed failure wedge makes an angle α with the horizontal. The weight of failure wedge is W . The horizontal and vertical inertia forces are Q_h and Q_v . C is the total cohesive force and C_a is the total soil-wall adhesion force. Soil-wall adhesion factor, a_f is equals to C_a/C or c_a/c , where c_a is the soil-wall adhesion.

From the Figure (1), at depth z the mass of the strip of thickness dz can be obtained as:

$$m(z) = \frac{\gamma}{g} m(\alpha)(H - z) dz \tag{1a}$$

where,

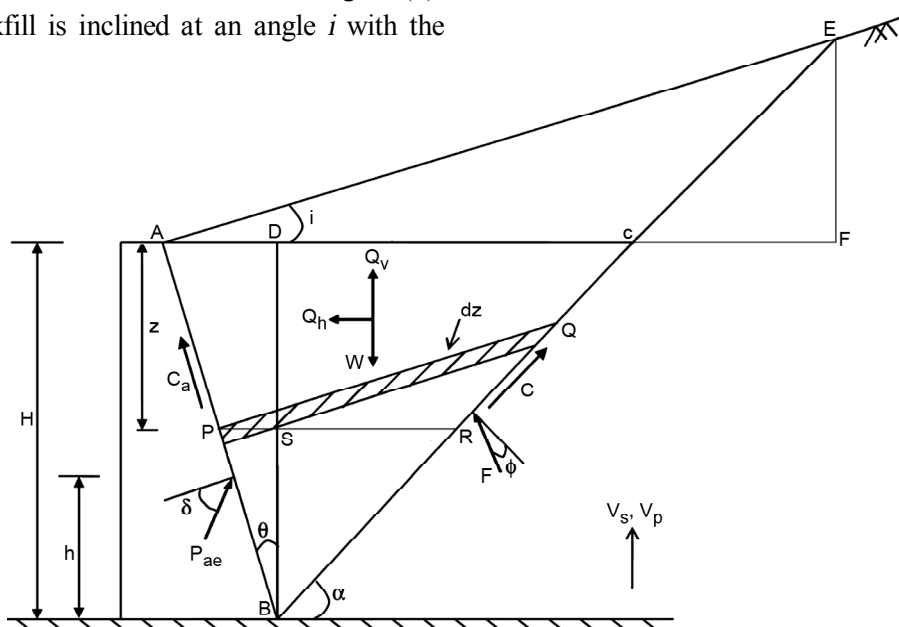


Figure 1. Forces acting on retaining wall in active state.

$$m(\alpha) = \frac{(1 + \tan \alpha \tan \theta) \sin \alpha \cos(\theta - i)}{\tan \alpha \sin(\alpha - i) \cos \theta} \quad (1b)$$

The weight of the failure wedge is obtained as:

$$W = \frac{1}{2} \gamma H^2 m(\alpha) \quad (2)$$

The horizontal and vertical acceleration at depth z below the top of the wall is expressed as:

$$a_h(z, t) = \left\{ 1 + \frac{H - z}{H} (f_a - 1) \right\} k_h g \sin \omega \left(t - \frac{H - z}{V_s} \right) \quad (3a)$$

$$a_v(z, t) = \left\{ 1 + \frac{H - z}{H} (f_a - 1) \right\} k_v g \sin \omega \left(t - \frac{H - z}{V_p} \right) \quad (3b)$$

The total horizontal and vertical inertia forces (Q_h and Q_v) acting in the failure wedge can be calculated as:

$$Q_h = \int_0^H m(z) a_h(z, t) dz \quad (4)$$

and

$$Q_v = \int_0^H m(z) a_v(z, t) dz$$

After integration of Equation (4), Q_h and Q_v can be expressed as:

$$Q_h = \frac{\lambda \gamma k_h m(\alpha)}{4\pi^2} \left[\left\{ 2\pi H \cos \omega \zeta \right. \right. \\ \left. \left. + \lambda (\sin \omega \zeta - \sin \omega t) \right\} + \frac{(f_a - 1)}{\pi H} \left\{ 2\pi H \left(\begin{matrix} \pi H \cos \omega \zeta \\ + \lambda \sin \omega \zeta \end{matrix} \right) \right. \right. \\ \left. \left. + \lambda^2 (\cos \omega t - \cos \omega \zeta) \right\} \right] \quad (5)$$

$$Q_v = \frac{\eta \gamma k_v m(\alpha)}{4\pi^2} \left[\left\{ 2\pi H \cos \omega \psi \right. \right. \\ \left. \left. + \eta (\sin \omega \psi - \sin \omega t) \right\} + \frac{(f_a - 1)}{\pi H} \left\{ 2\pi H \left(\begin{matrix} \pi H \cos \omega \psi \\ + \eta \sin \omega \psi \end{matrix} \right) \right. \right. \\ \left. \left. + \eta^2 (\cos \omega t - \cos \omega \psi) \right\} \right] \quad (6)$$

where,

$$\lambda = TV_s; \eta = TV_p; \zeta = \left(t - \frac{H}{V_s} \right) \text{ and } \psi = \left(t - \frac{H}{V_p} \right)$$

On resolving the forces in the horizontal and vertical direction on the failure wedge in the equilibrium condition, total seismic active earth pressure, P_{ae} can be obtained as:

$$P_{ae} = \left[\left\{ \frac{\{W - Q_v\} \sin(\alpha - \phi) + 2Q_h \cos(\alpha - \phi)}{\cos(\delta + \theta - \alpha + \phi)} \right\} \right. \\ \left. - cH \left\{ \frac{\{\cos(\theta - i) \cos \phi - a_f \sin(\theta - \alpha + \phi) \sin(\alpha - i)\}}{\sin(\alpha - i) \cos \theta \cos(\delta + \theta - \alpha + \phi)} \right\} \right] \quad (7)$$

Substituting the values of W , Q_h and Q_v in Equation (7), an expression for total seismic active earth pressure P_{ae} can be derived. Equation (7) is then optimized with respect to their two variables α and t/T , to obtain the maximum value of total seismic active earth pressure P_{ae} for the given wall and backfill combination subjected to ground motion with the soil amplification effect. Results can be normalized in the form of seismic active earth pressure coefficient K_{ae} as $K_{ae} = P_{ae} / (0.5\gamma H^2)$ for comparison.

On taking the partial derivative of P_{ae} with respect to z , seismic active earth pressure distribution behind the retaining wall can be determined by:

$$P_{ae} = \frac{\partial P_{ae}}{\partial z} \quad (8)$$

For $c-\phi$ soil backfill, depth of tension crack (z_c) can be determined, at where the value of seismic earth pressure P_{ae} will be zero. Considering the effect of tension crack, negative pressure in the top portion up to depth (z_c) can be neglected. Then, effective total seismic active earth pressure can be computed from integrating earth pressure P_{ae} from z_c to H . In such case, effective seismic active earth pressure coefficient can be defined as $K_{ae}^{zc} = P_{ae}^{zc} / (0.5\gamma H^2)$.

3. Results and Discussion

In the present study, a parametric study is conducted to examine the effect of various parameters such as ground motion parameters (k_h and k_v), soil cohesion, adhesion factor, wall friction

angle, wall and backfill inclination. To quantify the effect, seismic active earth pressure coefficient (K_{ae}), depth of tension crack (z_c), effective seismic active earth pressure coefficient due to depth of tension crack (K_{ae}^{zc}), and critical inclination of failure wedge (α_{cri}) are compared in tabular form. Geometrical properties of wall and material properties of backfill

considered in the present study are reported in Table (1).

3.1. Effect of f_a on K_{ae}

Table (2) compares the values of K_{ae} for the three combinations of c and a_f for the horizontal ($i = 0^\circ$) and for the inclined ($i = 10^\circ$) soil backfill

Table 2. Variation of parameters considered in the present study.

S. No.	Description	Values are Taken
1.	Unit Weight of Soil Backfill (γ)	20 kN/m ³
2.	The Height of Retaining Wall (H)	10 m
3.	Shear Wave Velocity (V_s)	100 m/s
4.	Primary Wave Velocity (V_p)	187 m/s
5.	The Time Period of Lateral Shaking (T)	0.3 s
6.	Soil Cohesion (c)	0.0 and 10 kPa
7.	Adhesion Factor (a_f)	0.0 and 1.0
8.	Soil Friction Angle (ϕ)	30°
9.	Wall inclination with the vertical (θ)	-30°, 0° and 30°
10.	The Inclination of Soil Backfill with the Horizontal (i)	0° and 10°
11.	Wall Friction Angle (δ)	0, 0.5 ϕ and ϕ
12.	Coefficient of Horizontal Seismic Acceleration (k_h)	0.0, 0.1, 0.2, 0.3 and 0.4
13.	Coefficient of Vertical Seismic Acceleration (k_v)	- k_h , -0.5 k_h , 0.0, 0.5 k_h , k_h
14.	Soil Amplification Factor (f_a)	1.0, 1.2, 1.4, 1.6 and 1.8

Table 2. Values of K_{ae} for different k_h ($H/\lambda = 0.333$; $H/\eta = 0.178$; $k_v = 0.5k_h$; $\delta = 0.5\phi$ and $\theta = 30^\circ$).

c (kPa)	a_f	i (°)	f_a	k_h				
				0.0	0.1	0.2	0.3	0.4
0	0	0	1.0	0.609	0.669	0.756	0.898	1.182
0	0	0	1.2	0.609	0.679	0.788	0.988	1.513
0	0	0	1.4	0.609	0.690	0.825	1.112	2.517
0	0	0	1.6	0.609	0.701	0.868	1.294	-----
0	0	0	1.8	0.609	0.713	0.919	1.600	-----
10	0	0	1.0	0.515	0.568	0.640	0.745	0.919
10	0	0	1.2	0.515	0.577	0.665	0.806	1.075
10	0	0	1.4	0.515	0.586	0.693	0.881	1.323
10	0	0	1.6	0.515	0.595	0.725	0.979	1.812
10	0	0	1.8	0.515	0.605	0.761	1.111	-----
10	1.0	0	1.0	0.501	0.565	0.654	0.782	0.992
10	1.0	0	1.2	0.501	0.576	0.684	0.855	1.176
10	1.0	0	1.4	0.501	0.587	0.718	0.946	1.466
10	1.0	0	1.6	0.501	0.599	0.757	1.063	2.023
10	1.0	0	1.8	0.501	0.611	0.800	1.218	-----
0	0	10	1.0	0.734	0.836	1.009	1.404	-----
0	0	10	1.2	0.734	0.854	1.082	1.870	-----
0	0	10	1.4	0.734	0.874	1.174	-----	-----
0	0	10	1.6	0.734	0.896	1.297	-----	-----
0	0	10	1.8	0.734	0.919	1.476	-----	-----
10	0	10	1.0	0.613	0.695	0.817	1.028	1.558
10	0	10	1.2	0.613	0.709	0.863	1.175	1.838
10	0	10	1.4	0.613	0.724	0.917	1.403	2.183
10	0	10	1.6	0.613	0.739	0.982	1.887	-----
10	0	10	1.8	0.613	0.756	1.061	2.191	-----
10	1.0	10	1.0	0.607	0.703	0.846	1.090	1.684
10	1.0	10	1.2	0.607	0.720	0.899	1.256	1.991
10	1.0	10	1.4	0.607	0.737	0.962	1.512	-----
10	1.0	10	1.6	0.607	0.755	1.036	2.043	-----
10	1.0	10	1.8	0.607	0.775	1.126	2.372	-----

for the range of the value of k_h are 0.0 to 0.4.

Case 1: $c=0$ and $a_f=0.0$

Case 2: $c=10$ kPa and $a_f=0.0$

Case 3: $c=10$ kPa and $a_f=1.0$

Soil amplification factor, f_a is taken as 1.0, 1.2, 1.4, 1.6 and 1.8. Other parameters are assumed as: $k_v = 0.5k_h$; $\delta = 0.5\phi$ and $\theta = 30^\circ$. From the Table (2), it can be clearly noticed that the value of K_{ae} increases significantly on increasing the values of soil amplification factor from 1.0 to 1.8 for all the three cases of assumed soil backfill. The effect of soil amplification is noticed significantly more for the value of $f_a > 1.4$. The effect of the inclination of soil backfill is also noticed clearly from Table (2). The values of K_{ae} are more for the inclined soil backfill for all the three assumed cases. For example, for horizontal soil backfill and $k_h=0.2$, increasing the value of f_a as 1.2 to 1.8 resulted the percentage increase in the values of K_{ae} with respect to $f_a = 1.0$ (no amplification) as 4.2, 9.1, 14.8, 21.5 (for Case 1); 3.9, 8.3, 13.3, 18.9 (for Case 2) and 4.6, 9.8, 15.8, 22.3 (for Case 3). The same percentage increase for the inclined ($i = 10^\circ$) soil backfill cases are 7.2, 16.4, 28.5, 46.3 (for Case 1); 5.6, 12.2, 20.2, 29.9 (for Case 2) and 6.3, 13.7, 22.5, 33.1 (for Case 3). It can be seen that on average 60% more increase in the values of K_{ae} are observed for inclined backfill case.

3.2. Effect of k_h on K_{ae}

The effect of k_h on the values of K_{ae} for all the three cases can be summarized from Table (2). As expected it increases continuously on increasing the values of k_h from 0.0 to 0.4. This can be attributed to the increase in the inertial force of failure wedge with ground acceleration. The value of K_{ae} is more

for the case of cohesionless soil backfill as compared with the cohesive soil backfill. The effect of k_h is also noticed more for the case of inclined soil backfill as compared with the horizontal soil backfill. For example, on increasing the k_h from static to dynamic case for the horizontal soil backfill for $c = 10$ kPa; $a_f = 0.0$; $f_a = 1.0$; $k_h = 0.1, 0.2, 0.3, 0.4$ and $k_v = 0.5k_h$; percentage increase in K_{ae} is 10.2, 24.2, 44.7 and 78.4.3 respectively. The same percentage increase is 13.7, 34.6, 71.1 and 156.9 for soil amplification factor $f_a = 1.4$. For the inclined ($i=10^\circ$) soil backfill, the same percentage increase is 13.3, 33.3, 67.7 and 154.2 respectively (for $f_a = 1.0$) and 18.1, 49.6, 128.9 and 256.1 respectively (for $f_a = 1.4$).

3.3. Effect of f_a and k_h on Depth of Tension Crack, z_c

Table (3) comprises the depth of tension crack, z_c for $c = 10$ kPa and $a_f = 1.0$. Other parameters are as: k_h (0.0, 0.1, 0.2, 0.3 and 0.4); f_a (1.0, 1.2, 1.4, 1.6 and 1.8); $k_v = 0.5k_h$; $\delta = 0.5\phi$; $\theta = 30^\circ$ and $i = 0^\circ$ and 10° . The value of z_c increases with soil amplification factor and horizontal seismic coefficient. For the inclined soil backfill, the effect is more pronounced as more increase in the value of z_c is noticed. For example, on increasing the k_h from 0.1 to 0.2, 0.2 to 0.3, 0.3 to 0.4 for the horizontal soil backfill; the percentage increase in the value of z_c are 1.17, 12.7 and 40.2 respectively for $f_a=1.0$. The same percentage increase is 3.52, 25 and 62.7 respectively for $f_a=1.2$. For the inclined ($i=10^\circ$) soil backfill the same percentage increase is 14.7, 43.5 and 84.1 (for $f_a=1.0$) and 22.2, 67.2 and 75.0 (for $f_a=1.2$).

For the value of $k_h = 0.3$, increasing the soil

Table 3. Values of depth of tension crack, z_c (m) for different k_h ($H/\lambda = 0.333$; $H/\eta = 0.178$; $k_v = 0.5k_h$; $\delta = 0.5\phi$ and $\theta = 30^\circ$).

c (kPa)	a_f	i (°)	f_a	k_h				
				0.0	0.1	0.2	0.3	0.4
10	1.0	0	1.0	0.88	0.85	0.86	0.97	1.36
10	1.0	0	1.2	0.88	0.85	0.88	1.10	1.79
10	1.0	0	1.4	0.88	0.85	0.92	1.30	2.35
10	1.0	0	1.6	0.88	0.85	0.97	1.59	3.06
10	1.0	0	1.8	0.88	0.86	1.04	1.95	-----
10	1.0	10	1.0	0.86	0.88	1.01	1.45	2.67
10	1.0	10	1.2	0.86	0.90	1.10	1.84	3.22
10	1.0	10	1.4	0.86	0.91	1.22	2.41	-----
10	1.0	10	1.6	0.86	0.93	1.39	3.35	-----
10	1.0	10	1.8	0.86	0.95	1.60	3.85	-----

amplification factor from 1.0 to 1.2, 1.4, 1.6 and 1.8; the respective percentage increase (with respect to $f_a = 1.0$ case) is 13.4, 34.0, 63.9 and 101.0 for the horizontal soil backfill. The same percentage is 26.8, 66.2, 131.0 and 165.5 for the inclined ($i = 10^\circ$) soil backfill. With the help of obtained z_c values, the corresponding values of K_{ae}^{zc} are reported in Table (4).

3.4. Effect of δ and θ on K_{ae}

The effect of δ and θ on K_{ae} are reported in Table (5) for $c = 10$ kPa and $a_f = 1.0$. Other parameters are as: $k_h = 0.2$; $k_v = 0.5k_h$; f_a (1.0, 1.2, 1.4, 1.6 and 1.8); $i = 10^\circ$; δ (0, 0.5ϕ and ϕ) and θ (-30° , 0 and 30°). The value of K_{ae} decreases for the value of wall friction angle, δ from its 0 to 0.5ϕ value for negative wall inclination. Whereas for the positive wall inclination, the value of K_{ae} continuously increases for the value of δ from 0° to ϕ . For example, for the assumed parameters for Table (5), on increasing the wall inclination θ from 0° to 30° ; f_a from 1.0, 1.2, 1.4, 1.6 and 1.8, the respective percentage increase in the value of K_{ae} is 129.7, 123.4, 117.0, 111.5, 107.1 (for $\delta = 0^\circ$); 160.3, 153.9, 149.2, 144.9, 142.1 (for $\delta = 0.5\phi$) and 210.2, 207.5, 205.8, 207.2, 210.6 (for $\delta = \phi$). From

the example, it can be noticed that the effect of wall inclination θ on K_{ae} is more critical as compared to the effect of f_a and δ .

3.5. Effect of δ and θ on α_{cri}

The effect of δ and θ on failure wedge angle α_{cri} are summarized in Table (6) for $c = 10$ kPa and $a_f = 1.0$. Other parameters are as: $k_h = 0.2$; $k_v = 0.5k_h$; f_a (1.0, 1.2, 1.4, 1.6 and 1.8); $i = 10^\circ$; δ (0° , 0.5ϕ and ϕ) and θ (-30° , 0 and 30°). The value of α_{cri} increases continuously for the wall inclination (from its negative to positive wall inclination), but decreases with the value of δ from its 0° to ϕ value. The value of α_{cri} decreases on increasing the value of soil amplification factor. For the values of the assumed parameters for Table (6), on increasing the wall inclination θ from -30° to 30° the respective percentage increments in the values of α_{cri} for $f_a = 1.0, 1.2$ and 1.4 , are 41.4, 38.3, 34.6 (for $\delta = 0^\circ$); 25.9, 22.5, 18.7 ($\delta = 0.5\phi$) and 11.0, 7.35, 3.35 ($\delta = \phi$). It is observed that effect of the wall inclination is reducing with the increase in soil amplification.

4. Validation of Results

The values of α_{cri} for different k_h and k_v ,

Table 4. Values of K_{ae}^{zc} for different k_h ($H/\lambda = 0.333$; $H/\eta = 0.178$; $k_v = 0.5k_h$; $\delta = 0.5\phi$ and $\theta = 30^\circ$).

c (kPa)	a_f	i (°)	f_a	k_h				
				0.0	0.1	0.2	0.3	0.4
10	1.0	0	1.0	0.602	0.675	0.783	0.959	1.329
10	1.0	0	1.2	0.602	0.688	0.822	1.079	1.745
10	1.0	0	1.4	0.602	0.701	0.871	1.250	2.505
10	1.0	0	1.6	0.602	0.716	0.928	1.503	4.198
10	1.0	0	1.8	0.602	0.731	0.997	1.880	-----
10	1.0	10	1.0	0.727	0.845	1.047	1.491	3.137
10	1.0	10	1.2	0.727	0.870	1.134	1.886	4.333
10	1.0	10	1.4	0.727	0.892	1.247	2.625	-----
10	1.0	10	1.6	0.727	0.918	1.396	4.623	-----
10	1.0	10	1.8	0.727	0.946	1.594	6.273	-----

Table 5. Values of K_{ae} for different δ and θ ($H/\lambda = 0.333$; $H/\eta = 0.178$; $k_h = 0.2$; $k_v = 0.5k_h$ and $i = 10^\circ$).

c (kPa)	a_f	f_a	$\delta = 0$			$\delta = 0.5\phi$			$\delta = \phi$		
			θ								
			-30°	0°	30°	-30°	0°	30°	-30°	0°	30°
10.0	1.0	1.0	0.019	0.336	0.772	0.017	0.325	0.846	0.016	0.340	1.055
10.0	1.0	1.2	0.047	0.362	0.809	0.041	0.354	0.899	0.039	0.373	1.147
10.0	1.0	1.4	0.077	0.392	0.851	0.068	0.386	0.962	0.065	0.412	1.260
10.0	1.0	1.6	0.111	0.425	0.899	0.098	0.423	1.036	0.094	0.456	1.401
10.0	1.0	1.8	0.148	0.462	0.957	0.132	0.465	1.126	0.128	0.509	1.581

Table 6. Values of $\alpha_{cri}(\circ)$ for different δ and θ ($H/\lambda = 0.333$; $H/\eta = 0.178$; $k_h = 0.2$; $k_v = 0.5k_h$ and $i = 10^\circ$).

c (kPa)	a_r	f_a	$\delta = 0$			$\delta = 0.5\phi$			$\delta = \phi$		
			θ								
			-30°	0°	30°	-30°	0°	30°	-30°	0°	30°
10.0	1.0	1.0	36.28	45.66	51.33	36.21	43.67	45.61	36.15	41.93	40.15
10.0	1.0	1.2	35.11	43.86	48.56	34.95	41.77	42.83	34.82	39.94	37.38
10.0	1.0	1.4	33.83	41.86	45.54	33.58	39.69	39.88	33.37	37.78	34.49
10.0	1.0	1.6	32.43	39.66	42.24	32.07	37.41	36.73	31.78	35.44	31.49
10.0	1.0	1.8	30.85	37.18	38.64	30.40	34.89	33.39	30.04	32.90	28.39

Table 7. Values of $\alpha_{cri}(\circ)$ for different k_h and k_v ($c = 0.0$; $\gamma = 18 \text{ kN/m}^3$; $H = 10 \text{ m}$; $V_p = 111.1 \text{ m/s}$; $V_s = 208.3 \text{ m/s}$; $T = 0.3 \text{ sec}$; $H/\lambda = 0.3$; $H/\eta = 0.16$; $\phi = 30^\circ$; $i = 5^\circ$; $\delta = 15^\circ$; $\theta = 5^\circ$).

k_h	k_v	Present Study			Xiao-bo et al. [11]			M-O Method
		$f_a = 1.0$	$f_a = 1.2$	$f_a = 1.4$	$f_a = 1.0$	$f_a = 1.2$	$f_a = 1.4$	
0.1	-0.1	52.28	51.59	50.91	52.14	51.43	50.71	51.67
0.1	-0.05	51.98	51.21	50.44	51.93	51.16	50.38	51.38
0.1	0	51.70	50.85	49.99	51.70	50.85	49.99	51.05
0.1	0.05	51.53	50.62	49.67	51.44	50.51	49.55	50.69
0.1	0.1	51.73	50.78	49.75	51.15	50.12	49.04	50.28
0.2	-0.2	47.26	45.88	44.48	46.93	45.48	44.01	46.16
0.2	-0.1	46.18	44.50	42.76	46.07	44.37	42.62	44.95
0.2	0	45.01	42.97	40.80	45.01	42.97	40.80	43.45
0.2	0.1	43.85	41.32	38.53	43.68	41.13	38.33	41.53
0.2	0.2	42.80	39.49	35.60	41.96	38.64	34.80	39.00

obtained in the present study have been compared with the values reported by Xiao-bo et al. [11] and M-O Method for a set of parameters ($c = 0.0$; $\gamma = 18 \text{ kN/m}^3$; $H = 10 \text{ m}$; $V_p = 111.1 \text{ m/s}$; $V_s = 208.3 \text{ m/s}$; $T = 0.3 \text{ sec}$; $H/\lambda = 0.3$; $H/\eta = 0.16$; $\phi = 30^\circ$; $i = 5^\circ$; $\delta = 15^\circ$; $\theta = 5^\circ$) in Table (7). On comparing the present results with Xiao-bo et al. [11], the values of α_{cri} obtained are in good agreement with average deviation of 0.57%. Similarly, the predicted values of K_{ac}^{zc} shown in Table (8), for different ϕ are compared with the results from Shao-jun et al. [10]. Parameters considered for comparison are as ($c = 10 \text{ kPa}$; $a_f = 0$; $\gamma = 18 \text{ kN/m}^3$; $H = 6 \text{ m}$; $V_p = 111.1 \text{ m/s}$; $V_s = 208.3 \text{ m/s}$; $T = 0.3 \text{ sec}$; $H/\lambda = 0.18$; $H/\eta = 0.096$; $i = 0^\circ$; $\delta = 0^\circ$; $\theta = 0^\circ$; $k_h = 0.2$; $k_v = 0.1$; $f_a = 1.0$). As different optimization procedure was considered for α_{cri} deviation in the predictions were observed.

Table 8. Values of K_{ac}^{zc} for different ϕ ($c = 10$; $a_f = 0$; $\gamma = 18 \text{ kN/m}^3$; $H = 6 \text{ m}$; $V_p = 111.1 \text{ m/s}$; $V_s = 208.3 \text{ m/s}$; $T = 0.3 \text{ sec}$; $H/\lambda = 0.18$; $H/\eta = 0.096$; $i = 0^\circ$; $\delta = 0^\circ$; $\theta = 0^\circ$; $k_h = 0.2$; $k_v = 0.1$; $f_a = 1.0$).

ϕ (°)	Present Study	Shao-Jun et al. [10]
20	0.578	0.390
30	0.396	0.250
40	0.260	0.170

5. Conclusions

In the present study, an expression for K_{ac} is reported for calculating the seismic active earth pressure behind the inclined retaining wall. The expression is obtained for the inclined cohesive soil backfill including the effect of soil amplification. Results indicated the non-linear behavior in the seismic earth pressure with ground acceleration parameters in the pseudo-dynamic approach, which shows the actual behavior of retaining wall under seismic condition. The main conclusions are as follows:

- ❖ On increasing the values of horizontal seismic coefficient, the value of K_{ac} increases significantly. The increase is more for the value of $k_h > 0.2$ for both cohesionless and cohesive soil.
- ❖ With the effect of soil amplification, the values of K_{ac} increases significantly. The effect of soil amplification is more for the values of f_a more than 1.4 for both cohesionless and cohesive soil. The effect of soil amplification reduces for the c-φ soil backfill.
- ❖ The percentage increase is significantly more for the inclined soil backfill than the horizontal soil backfill.

- ❖ The depth of tension crack increases when soil amplification factor increases for the c - ϕ soil backfill. The increase is more for the case of inclined soil backfill.
- ❖ On increasing the wall inclination for its negative to positive values, the value of K_{ae} increases significantly for the positive values of wall inclination for c - ϕ soil backfill.
- ❖ For negative wall inclination and sloping backfill, the value of K_{ae} decreases for the values of wall friction angle, δ from its 0° to 0.5ϕ value. While for the positive wall inclination and sloping backfill, the value of K_{ae} continuously increases for the value of δ from 0° to ϕ .
- ❖ The values of critical inclination of failure wedge, α_{cr} increases continuously for the inclined wall (from its negative to positive wall inclination) and sloping c - ϕ soil backfill, for the value of δ from 0° to ϕ .

References

1. Okabe, S. (1926) General theory of earth pressure and seismic stability of retaining wall and dam. *Journal of the Japanese Society of Civil Engineers*, **10**(6), 1277-1323.
2. Mononobe, N. and Matsuo, H. (1929) On the determination of earth pressures during earthquakes. *Proceedings of the World Engineering Congress*, Tokyo, Japan, **9**, 179-187.
3. Steedman, R.S. and Zeng, X. (1990) The influence of phase on the calculation of pseudo-static earth pressure on a retaining wall. *Geotechnique*, **40**(1), 103-112.
4. Choudhury, D. and Nimbalkar, S.S. (2005) Seismic passive resistance by pseudo-dynamic method. *Geotechnique*, **55**(9), 699-702.
5. Choudhury, D. and Nimbalkar, S.S. (2006) Pseudo-dynamic approach of seismic active earth pressure behind retaining wall. *Geotechnical and Geological Engineering*, Springer, **24**(5), 1103-1113.
6. Nimbalkar, S.S. and Choudhury, D. (2008) Effects of body waves and soil amplification on seismic earth pressure. *Journal of Earthquake and Tsunami*, **2**(1), 33-52.
7. Ghosh, P. (2008) Seismic active earth pressure behind a non-vertical retaining wall using pseudo-dynamic analysis. *Canadian Geotechnical Journal*, **45**, 117-123.
8. Gupta, A. and Sawant, V.A. (2018) Effect of soil amplification on seismic earth pressure using pseudo-dynamic approach. *International Journal of Geotechnical Engineering*, doi:10.1080/19386362.2018.1476803.
9. Ghosh, S. and Sharma, R.P. (2010) Pseudo-dynamic active response of non-vertical retaining wall supporting c - ϕ backfill. *Geotechnical and Geological Engineering*, Springer, **28**(5), 633-641.
10. Shao-Jun, M.A., Kui-Hua, W., and Wen-Bing, W.U. (2012) Pseudo-dynamic active earth pressure behind retaining wall for cohesive soil backfill. *Journal of Central South University*, Springer, **19**, 3298-3304, doi: 10.1007/s11771-012-1407-5.
11. Xiao-Bo, R., Ru-Liang, Y., and Shu-Lin, S. (2013) Analysis of seismic active earth pressure on retaining walls based on pseudo-dynamic method. *Journal of Highway and Transportation Research and Development*, ASCE, **7**(2), 34-39.